Inversion Motion and S_1 Equilibrium Geometry of 4-Fluoroaniline: Molecular Beam High-Resolution Spectroscopy and ab Initio Calculations

M. Becucci,* E. Castellucci, I. López-Tocón, G. Pietraperzia, and P. R. Salvi

LENS, Università di Firenze, Largo E. Fermi 2, I-50125 Firenze, Italy, and Dipartimento di Chimica, Università di Firenze, via G. Capponi 9, I-50121 Firenze, Italy

W. Caminati

Dipartimento di Chimica "G. Ciamician", Università di Bologna, via Selmi 2, I-40126 Bologna, Italy

Received: May 11, 1999; In Final Form: July 29, 1999

The fluorescence excitation spectrum in the region of the 0_0^0, $6a_0^1$, I_0^2 and 1_0^1 $S_1 \leftarrow S_0$ bands of 4-fluoroaniline expanded in a supersonic beam has been measured under high-resolution conditions with complete spectral resolution of the rotational components. The rotational constants of the four vibronic levels have been determined. The inversion motion in S_1 has been described by means of the flexible model approach, i.e., considering additional structural changes occurring in the molecule during the torsional oscillation. Structural relaxation is related to several internal coordinates, such as C_1N bond stretching, the HNH bending and the angular displacements from planarity. The equilibrium geometry of S_1, taking into account the present results and reported data, is found effectively planar with a barrier to inversion lower than 10 cm^{-1}. Excited-state rotational parameters such as the shifts of the planar moments of inertia justify satisfactorily the use of this model. Ab initio calculations with 6-31G basis sets including polarization and diffuse orbitals are in good agreement with the flexible model results, thus confirming the nonlocal character of the amino inversion in the excited state. The potential well has been also modeled ab initio for the ground-state including correlation effects through the perturbative MP2 treatment.

1. Introduction

The structure and dynamics of aniline and 4-fluoroaniline (4-FA) in the ground and first singlet excited state has attracted much attention in recent years, as they are prototype molecules for studying the interaction of the amino group with the aromatic ring.[1−12] The equilibrium geometry of both systems in the ground state is nonplanar, point group C_s, with the only symmetry element, the plane, normal to the benzene ring and through the nitrogen atom. The amino group is bent out of the cyclic structure with a dihedral angle of ≈46° between the NH_2 and ring planes according to vibrational and microwave data.[4−6] Further, from the analysis of the strongly anharmonic progression of the "umbrella"-like inversion mode, a barrier height of ≈600 cm^{-1} was calculated between the two equivalent C_s minima.[6]

The force field of the amino group changes with the electronic excitation. It has been in fact suggested that the regular spacing of the inversion levels in S_1 points for both molecules to a potential curve corresponding to a more planar structure than in the ground state.[1,2,7−12] Further, the inversion motion of aniline has been studied in detail, emphasizing the necessity of coupling the amino hydrogen motion with the C_1N bond stretching.[11] The rovibronic analysis was supported by calculations on the S_0 state and appropriate transfer to S_1.

In this paper high-resolution data are reported on several $S_1 \leftarrow S_0$ vibronic bands of 4-FA expanded in a supersonic molecular beam. The analysis of the experimental data is aimed at an improved determination of the S_1 equilibrium structure and at an accurate description of the inversion motion in the S_1 vibrational levels. The nonlocal character of the mode is effectively considered through the use of a flexible model,[13] i.e., taking into account the structural changes concurring with the amino hydrogen displacements out of the ring plane. Owing to the difficulty of the rigid model to reproduce rotational parameters in S_1, the flexible approach, widely applied with success in microwave spectroscopy, is proposed here to model not only vibrational spacings but also more subtle S_1 parameters, such as variations of the planar moments of inertia as a function of the vibrational level.

On the other hand, it is well-known that ab initio calculations give valuable information for comparison with observed structural data. Following this strategy, the equilibrium structure of pyridine in S_1 ($n\pi^*$) was found consistent with *a/b* axis switching upon excitation.[14] In the case of 4-FA the inversion potential well is represented with full optimization of the molecular structure at each torsional angle for both the ground and the excited S_1 states, using the 6-31G basis set, including polarization and diffuse orbitals. In addition, the influence of the electronic correlation is considered by applying the MP2 procedure to the RHF results.

The present interest in 4-FA is part of an extensive research activity of our group on amino aromatic species and their van der Waals complexes. As evidence has been accumulated on the special role of large amplitude motions in promoting predissociation processes in these species, we feel useful to address the issue by itself in 4-FA and to benefit from this background information to model subsequently the complex dynamics.

* Corresponding author. E-mail: becucci@lens.unifi.it.

10.1021/jp991554v CCC: $18.00
Published on Web 10/23/1999

2. Experimental Section

The 4-FA, purchased from Aldrich, was purified by vacuum distillation and stored at 5 °C in the dark. The experimental apparatus has been described in detail elsewhere.[15] Here we will give only a brief account of the present arrangement. The gas mixture used in the supersonic expansion was prepared by flowing helium over a reservoir of 4-FA kept at room temperature. The total gas pressure was about 400 kPa at the nozzle. The diameter of the nozzle and the skimmer were respectively 100 and 400 μm. The UV laser radiation was generated either intracavity, doubling the emission of a ring dye laser (single mode, frequency stabilized), or in an external cavity, resonant at the dye laser wavelength, for higher efficiency. The available UV laser power was respectively 1−2 or 8−10 mW for the two different setups. The total fluorescence emission from the excitation volume was collected with an efficient set of optics and measured with photon counting techniques.

Our laser spectrometer has an instrumental linewidth of 18 MHz in a practically Gaussian profile, mainly attributed to the Doppler broadening arising from the residual divergence of the molecular beam, as discussed in ref 15. The relative frequency scale of the spectra was initially provided by the use of a 150 MHz free spectral range étalon and refined by the use of the ground-state combination differences method relying on the microwave experimental data.[4] The absolute frequency was measured on a wavelength meter against the emission of a helium−neon laser with 600 MHz accuracy.

3. Experimental Results

In this work we present high-resolution rotational data on four different $S_1 \leftarrow S_0$ vibronic bands (0_0^0, $6a_0^1$, I_0^2, 1_0^1) of 4-FA expanded in a supersonic molecular beam. The bands have similar appearances suggestive of a *b* type transition of an asymmetric rotor with large energy gap. On the basis of this assumption as well as on the use of the rigid rotor Hamiltonian, simulated spectra have been fit to the experimental data by means of a nonlinear least-squares procedure. Rovibronic lines were assigned and rotational constants determined. The experimental and calculated spectra in the region of the $6a_0^1$ band are shown in Figure 1. The intensity distribution is reproduced assuming a Boltzmann population of the rotational states corresponding to 2.5 K and a linewidth of 60 MHz.

The experimental line profile has been fit to a Voigt function, the width of the Gaussian component being fixed by our instrumental linewidth (18 MHz) and the Lorentzian width freely adjusted. Within the experimental error, the same Lorentzian width (56 MHz fwhm) has been fit to each rovibronic transition. No power broadening effect was observed in the power range 1−10 mW available to the experiment. The measured Lorentzian linewidth corresponds to a fluorescence lifetime of 2.5 ns, independent of the particular rotational level of S_1 and of the vibrational energy excess. Also aniline has similar behavior with a longer lifetime, 7.9 ns.[11] The lifetime decrease with fluorine substitution is related to the larger vibronic density of states available for decay via ISC and/or IC in the 4-FA case. The relevant spectroscopic constants, such as band centers, upper state rotational constants, and inertial defects along the *c* axis are reported in Table 1.

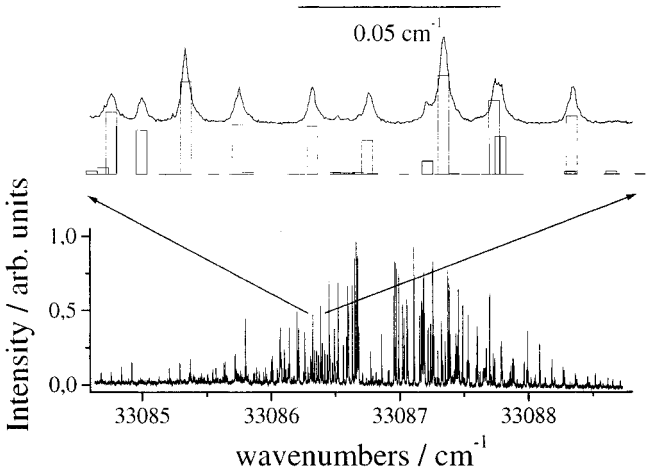

Figure 1. Spectrum of the jet-cooled 4-FA in the region of the $6a_0^1$ vibronic band. The expanded view in the upper part of the figure reports a small portion of the experimental and simulated (bar graph) spectrum showing complete rotational resolution.

4. Ab Initio Calculations

We performed several MO ab initio calculations using the GAUSSIAN 94[16] program package. The equilibrium geometries and energies of 4-FA in the ground state were calculated in the C_{2v} and C_s symmetry using the 6-31G basis set with polarization and diffuse orbitals. Correlation effects among electrons have also been considered by applying the MP2 corrections to the RHF results. The calculated barrier to inversion, taken as the difference between the energies of the C_{2v} and C_s structures at equilibrium, and the torsional equilibrium angle τ_0 change with the basis set and considering the electronic correlation. The results are reported in Table 2. It may be seen that the MP2 results, while closely approaching the experimental τ_0 value, slightly overestimate the inversion barrier.[6] On the whole, the 6-31$^+$G* results from RHF calculations are in fair agreement with reported values.[6] Further, the potential energy was evaluated as a function of the inversion mode by fully optimizing the molecular geometry at each CCNH dihedral angle. Excited-state wave functions were determined in the singly excited configuration interaction (CIS) scheme with a number of excited configurations equal to 3480. The S_1 state is predicted to be of $\pi\pi^*$ character, B_2 in C_{2v} symmetry (A″ in C_s). The S_1 equilibrium structures and energies were calculated in the C_{2v} and C_s symmetries, and the barrier to inversion was found ≤10

TABLE 1: Ground and Excited-State Spectroscopic Data[a] of 4-FA: Experimental Results

	0_0[b]	0^0	$6a^1$	I^2	1^1
ν_0 (cm^{-1})		32 653.54(4)	33 086.82(4)	33 426.24(4)	33 481.10(4)
A (cm^{-1})	0.186 605 0	0.175 368(4)	0.175 405(4)	0.175 061(4)	0.175 696(4)
B (cm^{-1})	0.048 337 4	0.049 379(1)	0.049 370(1)	0.049 316(1)	0.049 356(1)
C (cm^{-1})	0.038 431 9	0.038 548(1)	0.038 530(1)	0.038 531(1)	0.038 526(1)
no. assign		305	410	276	268
st dev (MHz)		10	12	15	13
Γ (MHz)		57(8)	55(6)	53(6)	58(9)
Δ (amu Å^2)	−0.4509	−0.2044	−0.0422	−0.6159	−0.0655

[a] Numbers in parentheses are one standard deviation in units of the last quoted decimal digit. [b] From ref 4.

TABLE 2: Calculated Ground-State Barrier ΔE (cm^{-1}) of 4-FA between Equilibrium C_{2v} and C_s Geometries and Torsional Angle τ_0 (degrees) in the C_s Structure as a Function of the Basis Set: RHF and MP2 Results

	basis set	ΔE	τ_0
RHF	6-31G*	658	45.0
	6-31$^+$G*	622	44.7
	6-31G**	534	43.6
	6-31$^+$G**	480	42.6
MP2	6-31G*	785	47.6
	6-31$^+$G*	763	46.0
	6-31G**	741	47.8
	6-31$^+$G**	711	45.3

TABLE 3: RHF/6-31$^+$G* Results on the S_0 State and CIS/6-31$^+$G* Results on the S_1 State of 4-FA: Equilibrium (C_s Symmetry) Structural Parameters[a] and Their Changes (Δ) Going to the Transition State (C_{2v} Symmetry)[b]

	S_0 state		S_1 state	
	C_s	Δ	C_s	Δ
C_1C_2	1.3923	0.0029	1.4249	0.0003
C_2C_3	1.3862	−0.0006	1.4049	0.0001
C_3C_4	1.3767	−0.0001	1.4000	−0.0002
C_2H	1.0762	0.0000	1.0740	0.0000
C_3H	1.0744	0.0001	1.0720	0.0000
C_1N (l)	1.4018	−0.0235	1.3409	−0.0027
NH	0.9983	−0.0064	0.9958	−0.0010
C_4F	1.3388	0.0018	1.3213	−0.0001
$C_1C_2C_3$	120.89	−0.03	118.83	−0.02
$C_2C_3C_4$	119.13	0.21	117.76	0.03
$C_2C_1C_6$	118.54	−0.17	121.95	−0.01
$C_3C_4C_5$	121.41	−0.19	124.87	−0.02
C_1C_2H	119.77	0.02	119.72	0.04
C_2C_3H	121.01	−0.17	122.53	−0.04
C_2C_1N	120.70	0.11	119.00	0.03
C_3C_4F	119.29	0.10	117.56	0.01
C_1NH	114.05	7.15	120.19	1.02
HNH (2α)	110.03	7.58	116.68	0.90
$C_3C_2-C_1C_6$	0.30	−0.30	−0.27	0.27
$C_2C_3-C_4C_5$	−0.07	0.07	0.12	−0.12
$C_4C_3-C_2H$	179.43	0.57	−178.95	−1.05
$C_1C_2-C_3H$	179.94	0.06	179.77	0.23
$C_2C_3-C_4F$	179.95	0.05	179.96	0.04

	S_0 state		S_1 state	
	C_s	C_{2v}	C_s	C_{2v}
τ	44.7	0	16.6	0
θ	2.6	0	2.4	0
ϕ	0.26	0	0.24	0
E	0	622	0	12

[a] Units: distances = angstrom, angles = degrees. [b] The relative energy (cm^{-1}) of the two molecular conformations and the values of the flexible model parameters in the two geometries are also given. See Figure 1.

cm^{-1} in all calculations. The structural results corresponding to the 6-31$^+$G* basis set are collected in Table 3.

5. Discussion

In previous papers the inversion mode of the 4-FA amino group was described as a local motion involving only the two amino hydrogens. The ground-state potential function was modeled as a double minimum well resulting from a harmonic potential and a Gaussian barrier.[6] A potential function resulting from quadratic and quartic contributions was suggested for the same mode in S_1.[8]

On the other hand, it was shown for aniline that an improved representation of the inversion motion in S_1 may be obtained by the following procedure.[11] First, the molecular structure is fully optimized (RHF/6-31G*) at several inversion angles and the rotational constants evaluated. Then, from the analysis of the inversion sequence in S_1 average angles for the 0^0 and I^2 levels are obtained and the associated rotational constants compared with those relative to the previous optimizations. The large discrepancy between calculated and observed S_1 inertial defects was attributed to inversion-induced changes occurring in S_1, notably the C_1N bond length.

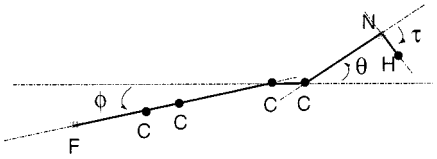

Figure 2. Schematic representation of 4-FA structure (C_s symmetry) projected on the symmetry plane (distances and angles are not in scale). The inversion angle τ and the angles θ and ϕ used in the flexible model are shown.

Following these considerations a more refined treatment is introduced here where, in addition to C_1N bond change, other molecular parameters vary as a result of the NH_2 torsional oscillation, i.e., the HNH angle and the angular displacements from planarity, θ and φ (see Figure 2). It is seen from ab initio data that these are among the parameters more directly related to inversion. Further, attempt is made to describe the inversion motion in the two states using the same potential function, combining vibrational and rotational information on the mode. In this approach vibrational energies and wave functions as well as rotational and centrifugal distortion constants are calculated starting from a given potential function. The leading coordinate for the inversion motion is the angle τ (see Figure 2), which is zero at planar molecular configuration. The following expansion of the potential energy in powers of the inversion angle is adopted

$$V(\tau) = p_1\tau^2 + p_2\tau^4 \tag{1}$$

which may be rewritten in a more meaningful form for a double minimum potential as

$$V(\tau) = B\left(1 - \left(\frac{\tau}{\tau_0}\right)^2\right)^2 \tag{2}$$

where B (cm^{-1}) gives directly the inversion barrier and τ_0 is the equilibrium inversion angle.[13,17] As the molecule is displaced along the torsional coordinate, the hybridization of the nitrogen atom changes from sp^3 (C_s symmetry) to sp^2 (C_{2v} symmetry). This results in molecular flexibility, i.e., in the change of other internal coordinates during the torsional motion. As anticipated, the structural relaxations are modeled as a function of the inversion angle τ as follows

$$\alpha(\tau) = \alpha_0 + \Delta\alpha(\tau/\tau_0)^2 \tag{3}$$

$$\theta(\tau) = \Delta\theta(\tau/\tau_0) \tag{4}$$

$$\phi(\tau) = \Delta\phi(\tau/\tau_0) \tag{5}$$

$$l(\tau) = l_0 + \Delta l(\tau/\tau_0)^2 \tag{6}$$

where 2α is the HNH angle, θ and ϕ are angular displacements from planarity (see Figure 2), and l is the C_1N bond length. The parameters α_0 and l_0 are the equilibrium values of the corresponding internal coordinates in planar configuration (for which $\theta = \phi = 0°$).

TABLE 4: RHF/6-31$^+$G Results on the S_0 State and CIS/6-31$^+$G** Results on the S_1 State of 4-FA: Equilibrium (C_s Symmetry) Structural Parameters[a] and Their Changes (Δ) Going to the Transition State (C_{2v} Symmetry)[b]**

	S_0 state		S_1 state	
	C_s	Δ	C_s	Δ
C_1C_2	1.3924	0.0027	1.4251	0.0001
C_2C_3	1.3861	−0.0005	1.4048	0.0000
C_3C_4	1.3765	−0.0002	1.3999	−0.0002
C_2H	1.0762	−0.0001	1.0739	0.0000
C_3H	1.0745	0.0001	1.0719	0.0000
C_1N (l)	1.3989	−0.0003	1.3397	−0.0015
NH	0.9962	−0.0062	0.9938	−0.0006
C_4F	1.339	0.0016	1.3212	−0.0001
$C_1C_2C_3$	120.88	−0.02	118.82	−0.01
$C_2C_3C_4$	119.13	0.19	117.74	0.02
$C_2C_1C_6$	118.54	−0.16	121.96	0.00
$C_3C_4C_5$	121.44	−0.18	124.92	−0.01
C_1C_2H	119.77	0.01	119.69	0.03
C_2C_3H	121.03	−0.16	122.58	−0.03
C_2C_1N	120.70	0.11	119.00	0.02
C_3C_4F	119.28	0.09	117.54	0.01
C_1NH	114.63	6.40	120.40	0.61
HNH (2α)	111.01	6.93	117.44	0.54
$C_3C_2-C_1C_6$	−0.27	0.27	−0.27	0.27
$C_2C_3-C_4C_5$	0.04	−0.04	0.15	−0.15
$C_4C_3-C_2H$	180.52	−0.52	179.26	0.74
$C_1C_2-C_3H$	179.93	0.07	180.16	−0.16
$C_2C_3-C_4F$	180.05	−0.05	179.93	0.07

	S_0 state		S_1 state	
	C_s	C_{2v}	C_s	C_{2v}
τ	42.6	0	13.0	0
θ	2.4	0	1.95	0
ϕ	0.23	0	0.23	0
E	0	480	0	6

[a] Units: distances = angstrom, angles = degrees. [b] The relative energy (cm^{-1}) of the two molecular conformations and the values of the flexible model parameters in the two geometries are also given. See Figure 1.

(a) Flexible Model Analysis of the Amino Inversion in S_0. At first we will discuss the properties of the inversion mode in the electronic ground state. Ab initio calculations provide the equilibrium geometry and the amplitude of the structural deformations during the inversion (Tables 3 and 4). Starting from RHF data and adjusting for best fit to the known vibrational spacings, the B and τ_0 parameters of Table 5 are obtained. It is seen that the B and τ_0 values from the 6-31$^+$G* and 6-31$^+$G** basis sets compare satisfactorily with experiment. On the other hand, a less reliable fit to the experimental frequency values is obtained from MP2 data. The structural relaxation parameters of eqs 3−6, determined from ab initio values at C_{2v} and C_s equilibrium geometries, are reported in Table 6. For both the S_0 and S_1 calculations in the flexible model approach the range $-90° < \tau < 90°$ has been resolved into 33 mesh points.[13]

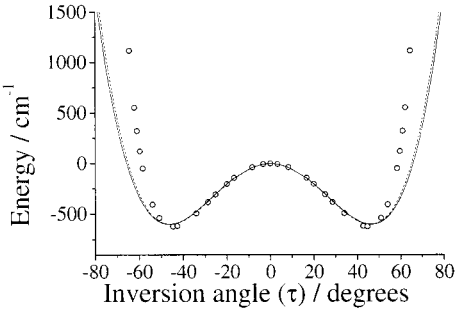

Figure 3. S_0 inversion potential curve: (circles) RHF/6-31$^+$G* results; (solid line) flexible model; (broken line) from ref 6.

In Figure 3 the potential curve obtained from this model is compared with that from a previous analysis[6] and with results from ab initio calculations (6-31$^+$G*). It may be seen that the two fitting procedures give consistent results each with the other. Also, the calculated barrier height and inversion angle are in close agreement with those of the two models. A discrepancy, however, exists in the shape of the potential curves for large inversion angles. All our ab initio calculations underestimate electronic interactions at these geometries. However, comparison of 6-31G results shows that basis enlargement and inclusion of electronic correlation reduce the gap beyond the torsional equilibrium angle.

It was not possible to test ab initio predictions on molecular flexibility, due to the lack of high-resolution rotational data on the S_0 inversion levels. In this regard experiments are in due course for a direct evaluation of the structural deformations and of the vibrational wave function at high v values of S_0.

(b) Electronic and Structural Differences between S_0 and S_1. The first allowed electronic transition of 4-FA has an excitation energy and intensity closely resembling that of other benzene derivatives and has been accordingly interpreted to be of $\pi\pi^*$ character. The first observed peak has been assigned as the 0_0^0 transition and classified of b type transition from band contour analysis. Therefore, the excited-state symmetry is B_2 in C_{2v} symmetry (or A″ in C_s). Our calculations agree with these symmetry species for S_1.

The analysis of our high-resolution spectra suggests a sizable change in the molecular structure toward planarity. Planar moments of inertia such as M_{aa}, related to the rotational constants by the following expression

$$M_{aa} = \sum_i m_i a_i^2 = h/(16\pi^2)\,(-1/A + 1/B + 1/C) \qquad (7)$$

(and similarly for M_{bb} and M_{cc}) are a measure of the mass extension along the principal inertia axes. They are reported in

TABLE 5: Inversion of the Amino Group in S_0: Vibrational Frequencies (cm^{-1}), Barrier Heights B (cm^{-1}), and Equilibrium Inversion Angles τ_0 (deg)

		calc freq			
	exp freq	flex mod RHF/6-31G*	flex. mod RHF/6-31$^+$G*	flex. mod RHF/6-31G**	flex. mod RHF/6-31$^+$G**
$\Delta E(I_1-0_0)$[a]	31.7	33.1	30.8	31.5	31.6
$\Delta E(I_2-0_0)$[a]	438.4	437.3	435.9	438.1	438.2
$\Delta E(I_3-0_0)$[a]	679.9	685.1	676.1	681.0	681.4
		Inversion Parameters			
B		590	600	600	600
τ_0	46[b]	46	46.5	46.5	46.5

[a] From ref 8. [b] From microwave data.[4]

TABLE 6: Structural Relaxation (Eqs 3−6) upon Amino Group Inversion in the S_0 and S_1 States[a]

	S_0		S_1			
	ab initio RHF/6-31$^+$G*	ab initio RHF/6-31$^+$G**	ab initio CIS/6-31$^+$G*	flex mod	ab initio CIS/6-31$^+$G**	flex mod
$\Delta\alpha$	−3.79	−3.47	−0.45	−0.62	−0.27	−0.39
$\Delta\theta$	2.6	2.4	2.43	2.12	1.95	1.8
$\Delta\phi$	0.26	0.2	0.24	0.22	0.23	0.26
Δl	0.0235	0.0203	0.0027	0.0031	0.0015	0.0020

[a] Units: distances = angstrom; angles = degrees.

TABLE 7: Planar Moments of Inertia (amu Å^2) in the Vibrational Ground Level of the S_0 and S_1 States

	S_0	S_1	Δ^a
M_{aa}	348.524	341.290	−7.234
M_{bb}	90.111	96.025	5.914
M_{cc}	0.228	0.102	−0.126

[a] $\Delta = M_{ii}(S_1) - M_{ii}(S_0)$.

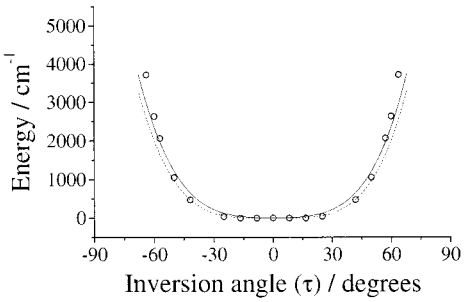

Figure 4. S_1 inversion potential curve: (circles) CIS/6-31$^+$G** results; (solid line) flexible model fit to 4-FA; (broken line) flexible model fit to 4-FA-D2.

Table 7 for the S_0 and S_1 ground levels of 4-FA. It is easy to see that the molecule considerably shortens along the *a*-axis and elongates along the *b*-axis going from S_0 to S_1 states. The inertial defect ($\Delta = -2M_{cc}$) of the ground vibrational state changes from −0.45, in S_0, to −0.20 amu Å^2, in S_1 (see Table 1). This corresponds to a change of the *effective* out-of-plane angle of the amino group from 46° to ≈20°, assuming that the deviation from planarity is due to the amino hydrogens only. The rotational constants of the other vibronic bands are consistent with the nature of the excited vibrational mode. The inertial defect of the $6a^1$ and 1^1 levels is sensibly increased with respect to that of the 0^0 level, as expected for in-plane vibrations. In the case of the I^2 level this quantity becomes much larger and negative, as should be for an out-of-plane, large amplitude, motion.

(c) Flexible Model Analysis of the Amino Group Inversion in the S_1 State. The flexible model approach has been extended to the inversion motion in S_1, considering the vibrational data[8] of 4-FA and of the molecule deuterated on the amino hydrogens (4-FA-D_2) and our rotational data from 0_0^0 and I_0^2 band contours. Starting from the calculated S_1 structure (C_{2v} symmetry, 6-31$^+$G**) as a reference configuration (see Table 4) and assuming the potential as in eq 1, the curve of Figure 4 has been derived through a fitting procedure to spectroscopic data. The potential is essentially flat for an inversion range −20°, +20° with respect to the planar C_{2v} structure. The amino hydrogens are free to move above and below the plane of the aromatic ring, with a root-mean-square linear displacement of ≈0.6 Å in the $v = 0$ level of S_1. This conclusion is in excellent agreement with CIS results. The calculated S_1 structure of 4-FA is almost planar, with a barrier height (<10 cm^{-1}) effectively zero within the calculation accuracy. The CIS energy data have been reported for comparison on Figure 4. Since the two sets of data are substantially independent of each other (except for the use of a reference structure based on ab initio data), their good agreement strongly supports an effective planarity of 4-FA in S_1. Equivalent results are obtained applying the same procedure to 6-31$^+$G* structural data.

TABLE 8: Experimental and Calculated Sequences of the Inversion (*I*) Progression in the S_1 State: Vibrational Frequencies (cm^{-1}), Second Moments of Inertia ΔM_{ii} (amu Å^2), and the Adopted Potential Functions $V(\tau)$

		calculated			
		CIS/6−31$^+$G*		CIS/6−31$^+$G**	
	exp	rigid mod	flex mod	rigid mod	flex mod
		4-FA			
$\Delta E(I^1\text{-}0^0)^a$	347	348.5	349.1	347.3	347.7
$\Delta E(I^2\text{-}0^0)^a$	772	770.5	771.1	769.4	770.3
$\Delta E(I^3\text{-}0^0)^a$	1235	1241.0	1234.5	1241.2	1236.0
$\Delta M_{aa}{}^b$	0.230	−0.872	0.228	−0.874	0.227
$\Delta M_{bb}{}^b$	−0.037	0.004	−0.059	0.0053	−0.055
$\Delta M_{cc}{}^b$	0.206	0.103	0.132	0.102	0.133
$V(\tau) = p_1\tau^2 + p_2\tau^4$					
$P_1{}^c$		0.118	0.100	0.110	0.105
$10^{-4}P_2{}^d$		0.90	1.3	0.89	1.53
		4-FA-D_2			
$\Delta E(I^2\text{-}0^0)^a$	572	573.1	572.4	572.1	571.4
$\Delta E(I^3\text{-}I^1)^a$	682	682.5	682.4	682.6	682.8
$V(\tau) = p_1\tau^2 + p_2\tau^4$					
$P_1{}^c$		0.06	0.003	0.055	0.0
$10^{-4}P_2{}^d$		1.63	1.46	1.6	1.55

[a] From ref 8. [b] $\Delta M_{ii} = M_{ii}(v = 2) - M_{ii}(v = 0)$ ($i = a, b, c$). [c] Units: cm^{-1} deg^{-2}. [d] Units: cm^{-1} deg^{-4}.

The flexible model approach is satisfactorily justified when the planar moments of inertia of the inversion levels $v = 0$ and $v = 2$ of S_1 are considered (see Table 1). The experimental and calculated variations [$\Delta M_{ii} = M_{ii}(v = 2) - M_{ii}(v = 0)$] in the S_1 state, reported in Table 8, agree in both sign and magnitude, reinforcing previous conclusions. On the contrary, a rigid model calculation, limited to out-of-plane displacements of the amino hydrogens, while able to predict correctly the observed vibrational spacings, is inadequate for the calculation of parameters of the S_1 state such as ΔM_{ii} ($i = a, b, c$) (see Table 8). This is direct evidence of the nonlocal nature of the inversion mode in the S_1 state. It may be seen, however, from Table 8 that, although the flexible model gives a ΔM_{cc} value in better agreement with experiment than the rigid model, a difference still exists with the observed ΔM_{cc} values. This means that the molecule has in the $v = 2$ level of the S_1 inversion mode a deviation from planarity on the average larger than predicted. It is plausible to attribute the effect to additional structural relaxations not considered in the present calculation. For the sake of simplicity, only the internal coordinates more directly involved in the structural relaxation have been considered in the present paper.

6. Summary

In this paper an experimental study of rovibronic S_1 levels of 4-FA is presented with complete rotational resolution. Combining our high-resolution data and accurate ab initio calculations with existing results on vibrational levels of the inversion mode, we have determined the shape of the potential surface along the inversion coordinate in the flexible model approach. The model has been tested on the S_0 potential curve. The S_1 potential presents a flat-bottomed shape for the inversion motion without a well-defined minimum between $-20°$ and $+20°$. The S_1 curve is also consistent with the inversion levels measured on a different isotopic species. The unusual shape accounts for previous interpretations of the large negative inertial defect of the 0^0 level in terms of a nonplanar equilibrium structure.[2]

Acknowledgment. This work was supported by the Italian MURST and by EU under Contracts No. CHRX-CT-0561, ERBFMBICT961046, ERBCHRXCT930105, and ERBFMG-ECT950017. I.L.T. acknowledges the Spanish Ministerio de Educacion y Ciencia for grant no. PF97/28482592. We acknowledge J. C. Otero for helpful discussions.

References and Notes

(1) Christoffersen, J.; J. M. Hollas, J. M.; Kirby, G. H. *Mol. Phys.* **1969**, *16*, 441.

(2) Christoffersen, J.; J. M. Hollas, J. M.; Kirby, G. H. *Mol. Phys.* **1970**, *18*, 451. Cvitaš, T.; Hollas, J. M.; Kirby, G. H. *Mol. Phys.* **1970**, *19*, 305.

(3) Lister, D. G.; Tyler, J. K. *Chem. Commun.* **1966**, 152. Lister, D. G.; Tyler, J. K.; Høg J. H.; Wessel Larsen, N. *J. Mol. Struct.* **1974**, *23*, 253.

(4) Hastie, A.; Lister, D. G.; McNeil, R. L.; J. K. Tyler, J. K. *Chem. Commun.* **1970**, 108.

(5) Larsen, N. W.; Hansen, E. L.; Nicolaisen, F. M. *Chem. Phys. Lett.* **1976**, *43*, 584.

(6) Kidd, R. A.; Krueger, P. J. *J. Chem. Phys.* **1978**, *69*, 827.

(7) Mikami, N.; Hiraya, A.; Fujiwara, I.; Ito, M. *Chem. Phys. Lett.* **1980**, *74*, 531.

(8) Gordon, R. D.; Clark, D.; Crawley, J.; Mitchell, R. *Spectrochim. Acta* **1984**, *40A*, 657.

(9) Tembreull, R.; Dunn, T. M.; Lubmann, D. M. *Spectrochim. Acta* **1986**, *42A*, 899

(10) Kerstel, E. R. Th.; Becucci, M.; Pietraperzia, G.; Consalvo, D.; Castellucci, E. *J. Mol. Spectrosc.* **1996**, *177*, 74.

(11) Sinclair, W. E.; Pratt, D. W. *J. Chem. Phys.* **1996**, *105*, 7942.

(12) Tseng, W. B.; Narajanan, K.; Hsieh, C. Y.; Tung, C. C. *J. Chem. Soc., Faraday Trans.* **1997**, *93*, 2981.

(13) Meyer, R. *J. Mol. Spectrosc.* **1979**, *76*, 266. Meyer, R.; Caminati, W. *J. Mol. Spectrosc.* **1991**, *150*, 229.

(14) Becucci, M.; Lakin, N. M.; Pietraperzia, G.; Salvi, P. R.; Castellucci, E. *J. Chem. Phys.* **1997**, *107*, 10399.

(15) Kerstel, E. R. Th.; Becucci, M.; Pietraperzia, G.; Castellucci, E. *Chem. Phys.* **1995**, *199*, 263.

(16) Frisch, M. J.; Trucks, G. W.; Schlegel, H. B.; Gill, P. M. W.; Johnson, B. G.; Robb, M. A.; Cheeseman, J. R.; Keith, T.; Petersson, G. A.; Montgomery, J. A.; Raghavachari, K.; M. Al-Laham, M. A.; Zakrzewski, V. G.; Ortiz, J. V.; Foresman, J. B.; Cioslowski, J.; Stefanov, B. B.; Nanayakkara, A.; Challacombe, M.; Peng, C. Y.; Ayala, P. J.; Chen, W.; Wong, M. W.; Andres, J. L.; Replogle, E. S.; Gomperts, R.; Martin, R. L.; Fox, D. J.; Binkley, J. S.; Defrees, D. J.; Baker, J.; Stewart, J. P.; Head-Gordon, M.; Gonzalez, C.; Pople, J. A. *Gaussian 94*, Revision E.2; Gaussian, Inc.: Pittsburgh, PA, 1995.

(17) Favero, L. B.; Corbelli, G.; Velino, B.; Caminati, W.; Favero, P. G. *Chem. Phys.* **1998**, *228*, 219.